Available online at www.sciencedirect.com

ScienceDirect

Ciência & Tecnologia dos Materiais 26 (2014) 1–8

Ciência & Tecnologia dos MATERIAIS

http://ees.elsevier.com/ctmat

# Emission of airborne ultrafine particles during welding of steel plates

J. F. Gomes[a,b*], R. M. Miranda[c]

[a]*IBB / Instituto Superior Técnico – Universidade de Lisboa, Av. Rovisco Pais, 1049-001 Lisboa, Portugal*
[b]*ADEQ, ISEL – Instituto Superior de Engenharia de Lisboa , R. Conselheiro Emídio Navarro, 1959-007 Lisboa, Portugal*
[c]*UNIDEMI, DEMI, Faculdade de Ciências e Tecnologia, FCT, Universidade Nova de Lisboa, 2829-516 Caparica, Portugal*

**Abstract**

The present study is focused on the characterization of ultrafine particles emitted in welding of steel using mixtures of Ar+$CO_2$, and intends to analyze which are the main process parameters which may have influence on the emission itself. It was found that the amount of emitted ultrafine particles (measured by particle number and alveolar deposited surface area) are clearly dependent from the distance to the welding front and also from the main welding parameters, namely the current intensity and heat input in the welding process. The emission of airborne ultrafine particles seem to increase with the current intensity as fume formation rate does. When comparing the tested gas mixtures, higher emissions are observed for more oxidant mixtures, that is, mixtures with higher $CO_2$ content, which result in higher arc stability. The later mixtures originate higher concentrations of ultrafine particles (as measured by number of particles by $cm^3$ of air) and higher values of alveolar deposited surface area of particles, thus resulting in a more hazardous condition regarding worker's exposure.


*Keywords:* arc welding; welding fumes; ultrafine particles; alveolar deposited surface area.

## 1. Introduction

Arc welding is extensively used in metallic construction worldwide. However, it can produce dangerous fumes that may be hazardous to the welder's health [1] and it is estimated that, presently, 1-2% of workers from different professional backgrounds (which accounts for more than 3 million persons) are subjected to welding fume and gas action [2]. These authors also showed a correlation between processing parameters in metal active gas (MAG), that is, metal transfer modes, and the quantity of fumes formed expressed as fume formation rate. Additionally, the gas mixtures have also an influence on fumes (quantity and composition), since the higher the oxygen content of the gas, the higher the fume formation observed. With the advent of new types of welding procedures and consumables, the number of welders exposed to welding fumes is growing constantly, in spite of the mechanization and automation of the processes [3]. Simultaneously, the number of publications on epidemiologic studies [4] and the devices for welders' protection is also increasing. Apart from that, the influence of ultrafine particulate, lying in the nano range, on human health has been pointed to be of much concern [5-7] as airborne ultrafine particles can also result from macroscopic common industrial processes such as welding [8-9]. The detrimental health effects of inhaling ultrafine aerosols were recognised long ago and various attempts have been made to minimise exposure, as the issuing of specific regulations on emissions and objectives for air quality in working microenvironments.

When considering human exposure to airborne pollutants the exposure to airborne particles, and specifically to its finer fractions, such as sub micrometer particles, is of particular interest. Current workplace exposure limits, that have been established long ago, are based on particle mass, but this criteria

* Corresponding author.
*E-mail address*: jgomes@deq.isel.ipl.pt (J.F. Gomes)


http://dx.doi.org/10.1016/j.ctmat.2014.09.001

could not be completely adequate in what concerns nano sized particles as these materials are, in fact, characterized by very large surface areas (considering the same volume, nano sized particles have larger surface areas than micro sized particles, for instance), which has been pointed out as the distinctive characteristic that could even turn out an inert substance into a toxic one, but having the same chemical composition, and exhibiting very different interactions with biological fluids and cells [10-11]. As a result, assessing workplace conditions and personal exposure based on the measurement of particle surface area is of increasing interest. It is well known that lung deposition is the most efficient way for airborne particles to enter the body and potentially cause adverse health effects. If ultrafine particles can deposit in the lung and remain there, have an active surface chemistry and interact with the body, then, there is potential for exposure and dosing. Oberdörster [12] showed that surface area plays an important role in the toxicity of nanoparticles and is the measurement metric that best correlates with particle-induced adverse health effects. Therefore, in order to be able to assess exposure, it is important to have an estimation of the surface area of emitted ultrafine particles, as they are potentially able to deposit in the lower parts of the lung, such as the alveoli and clog them, or even being transferred to the blood circulation system with resulting distribution in several end organs [13].

In 1996, the International Commission of Radiological Protection (ICRP) developed a comprehensive lung deposition model for radioactive aerosols. Several parameters are required to construct the model including breathing rate, lung volume, activity, nose/mouth breathing, etc., and the obtained deposition curves (for tracheobronchial and alveolar deposition) derived from the model can vary according to these parameters. For industrial hygiene applications, ACGIH [14] developed a definition of a reference worker, in order to derive the corresponding deposition curves for tracheobronchial and alveolar lung deposition, based on the ICRP model: the tracheobronchial deposition curve represents the fraction of aerosol that deposits in the tracheobronchial region of the lung, while the alveolar deposition curve represents the fraction of the aerosol that deposits in the alveolar region of the lung. For exposure assessment applications it is common to sample aerosols relevant to their deposition in a specific region of the human lung thus depending on the aerosol being sampled. In what concerns ultrafine particles, due to its very fine dimensions, the health effects would be related to the deposition deep in the alveolar regions of the lung, so the respirable fraction of the aerosol is the metric of interest, as it is interesting to assess the potential surface of the alveoli to be clogged by the presence of these ultrafine particles.

This work comes in line with preliminary work from these authors that demonstrated the presence of ultrafine particles in welding processes such as metal-active gas (MAG) [4, 15], and aims to assess the emissions of ultrafine particles emitted from welding of steel and try to correlate these with operational parameters and, thus, molten metal transfer modes. Similar studies have also been made for welding fumes generated in other processes, such as manual metal arc welding (MMA), metal inert gas welding (MIG) and tungsten inert gas welding (TIG) for stainless steel electrodes [16]. Also, previous studies have not been assessing the deposited surface area of emitted particles.

## 2. Experimental

MAG welding tests were performed in laboratory using an experimental set-up consisting of an automatic welding machine Kemppi, model ProMig 501, controlled, which assured a stable electric arc, a constant welding speed and, therefore, repeatability of the welding process.

Bead on plate welds were performed on 3 mm thick mild carbon steel plates S235 JR with the chemical composition shown in table 1. Tests were also performed on austenitic 10 mm thick stainless steel plates AISI 304 having the chemical composition also shown in table 1. Welding consumables used were a solid wire AWS 5.18 ER79S-6, with a diameter of 1 mm for carbon steel and a solid wire AWS ER316 LSi, with a diameter of 0.8 mm, for stainless steel. Both solid wire compositions are shown in table 2.

The operating parameters used are depicted in table 3 for carbon steel and in table 4 for stainless steel. Different conditions were tested for welding, varying the gas protection mixture and current intensity and voltage in order to produce short-circuit, globular and spray metal transfer modes. The welding voltage was adjusted automatically by the welding machine in accordance with the feeding wire speed. Each test condition was replicated twice. Between each test, time intervals were provided in order to allow for some dissipation of aerosol in the closed atmosphere of the sampling location.

Table 1. Chemical composition of the base materials under study (wt. %)

| Steel | C | Mn | P | S | Si | Ni | Cr |
|---|---|---|---|---|---|---|---|
| AISI1020 | 0.017 | 1.40 | 0.035 | 0.035 | - | - | - |
| AISI304 | 0.08 | 2.0 | 0.045 | 0.030 | 0.75 | 8.0-10.5 | 18-20.0 |

Table 2. Chemical composition of the solid wire used (wt. %)

| Wire | C | Mn | P | S | Si | Ni | Cr |
|---|---|---|---|---|---|---|---|
| AWS 5.18 ER70S-6 | 0.06 - 0.15 | - | | 0.35 | 0.8-1.15 | 0.15 | 0.15 |
| AWS A5.9 ER316 LSi | 0.03 | 1.0-2.5 | 0.03 | 0.03 | 0.65-1.00 | 11-14 | 18-20 |

Gas protection was selected between industrial mixtures most frequently used, that generate high quantities of welding fume [17], which means high quantities of carbon dioxide and oxygen to improve penetration and bead width. Molten metal transfer modes were also chosen as the ones that produce high quantities of welding fume, between the more used in welding [17]. All welding tests were performed in the flat position. The gaseous mixtures were supplied by Air Liquide.

In order to assess the emissions of ultrafine particles on the nearby welding environment, sampling (using NSAM) was done as depicted in figure 1.

Table 3. Experimental test conditions for mild steel gas metal arc welding

| Gas mixture | ARCAL 21 (Ar + 10% $CO_2$) | | |
|---|---|---|---|
| Test nr. | 1 | 2 | 3 |
| Wire feed rate (m/min) | 4.0 | 6.3 | 11.2 |
| Intensity (A) | 102 | 137 | 194 |
| Voltage (V) | 17.8 | 20.0 | 32.4 |
| Metal transfer mode | Short-circuit | Globular | Spray |
| Gas mixture | ATAL 5 (Ar + 18% $CO_2$) | | |
| Test nr. | 1 | 2 | 3 |
| Wire feed rate (m/min) | 4.0 | 6.3 | Not attained |
| Intensity (A) | 92 | 122 | - |
| Voltage (V) | 17.7 | 19.9 | - |
| Metal transfer mode | Short-circuit | Globular | Spray |
| Gas mixture | $CO_2$ | | |
| Test nr. | 1 | 2 | 3 |
| Wire feed rate (m/min) | 5.0 | 7.5 | Not attained |
| Intensity (A) | 64 | 129 | - |
| Voltage (V) | 18.7 | 21.1 | - |
| Metal transfer mode | Short-circuit | Globular | Spray |

Note: transfer modes classification is according to the International Institute of Welding (IIW) classification [18] and was verified, apart from welding parameters and other operational conditions combination described in this table, by observation of the electric arc length.

Table 4. Experimental test conditions for stainless steel gas metal arc welding

| Gas mixture | ARCAL 129 (Ar + 5% $CO_2$) | | |
|---|---|---|---|
| Test nr. | 1 | 2 | 3 |
| Wire feed rate (m/min) | 5.0 | 7.0 | 9.0 |
| Intensity (A) | 92 | 182 | 211 |
| Voltage (V) | 18.9 | 25.0 | 30.2 |
| Transfer mode | Short-circuit | Globular | Spray |
| Gas mixture | ARCAL 121 (Ar + 18% He + 1% $CO_2$) | | |
| Test nr. | 1 | 2 | 3 |
| Wire feed rate (m/min) | 5.0 | 7.0 | 9.0 |
| Intensity (A) | 133 | 171 | 199 |
| Voltage (V) | 18.8 | 25.0 | 29.9 |
| Transfer mode | Short-circuit | Globular | Spray |
| Gas mixture | ARCAL 12 (Ar + 5% He + 2% $CO_2$ + 2% $N_2$) | | |
| Test nr. | 1 | 2 | 3 |
| Wire feed rate (m/min) | 6.0 | 7.0 | 9.8 |
| Intensity (A) | 109 | 185 | 226 |
| Voltage (V) | 19.1 | 25.2 | 30.8 |
| Transfer mode | Short-circuit | Globular | Spray |

Note: the same note of Table 4 applies.

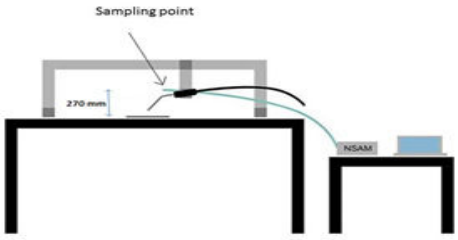


Fig. 1. Location of the sampling point.

During sampling, exhaustion was turned off, and doors and windows to the workshop were kept closed. For measuring ultrafine particle exposure a Nanoparticle Surface Area Monitor (NSAM), TSI, Model 3550, was used. This equipment estimates the human lung-deposited surface area of particles (ADSA) expressed as square micrometers per cubic centimeter of air ($\mu m^2/cm^3$), corresponding to the alveolar region of the lung. The operation of this equipment is based on diffusion charging of sampled particles (regardless of its size, shape and agglomeration, as discussed by Gomes [4], followed by detection of the charged aerosol using an electrometer, as described elsewhere [15]. It estimates the surface area of ultrafine particles capable of being deposited in the alveolar region of the lung, using the deposition model of ACGIH [14] previously mentioned. Due to the inexistence of an exposure limit value specific for ultrafine particles, for each measurement task a baseline value was obtained for comparison purposes.

Particles were also collected using a Nanometer Aerosol Sampler (NAS), TSI, Model 3089, on 3mm diameter copper grids polymer coated for further observation by transmission electron microscopy (TEM), Hitachi, model H-8100 II, equipped with an energy dispersive X-ray spectroscopy (EDS) probe.

## 3. Results and discussion

The measured data for each welding tests are depicted in the next figures as follows: figures 2 to 4 referring to carbon steel, and figures 5 to 7 to stainless steel. In each one, the top figure represents the measured ADSA, expressed as square micrometers per cubic centimeter of air ($\mu m^2/cm^3$), corresponding to the alveolar region of the lung versus welding time, for each welding transference mode (short-circuit, globular and spray).

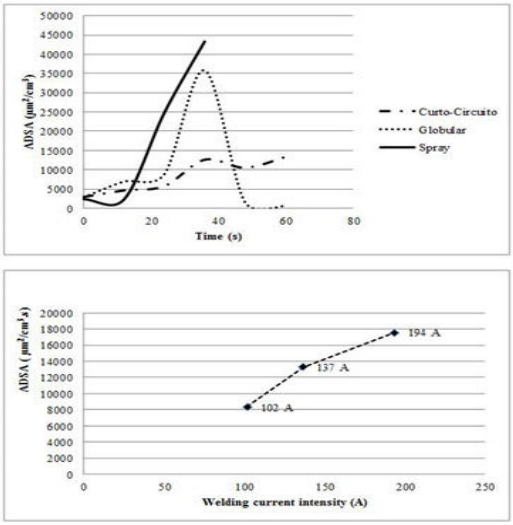


Fig. 2. Results for welding tests with ARCAL 21.

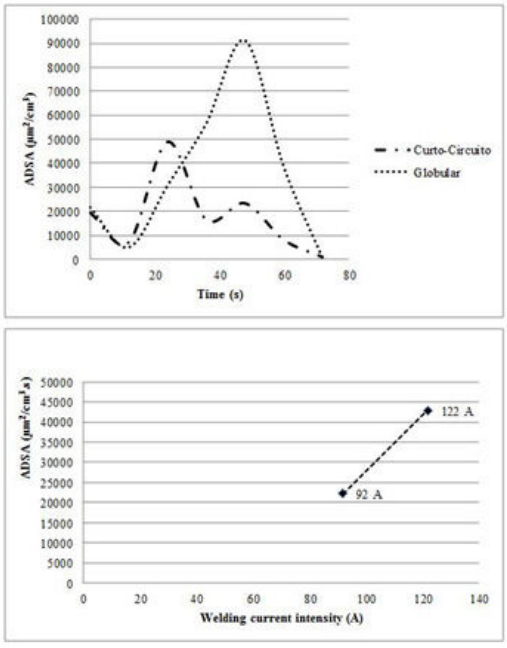


Fig. 3. Results for welding tests with ATAL.

The bottom figure represents ADSA versus the applied welding current intensity.

It should be noted that these graphs show, not the instantaneous ADSA, but the integrated curves for the whole welding period, which means that the graphs show the acumulated ADSA for the whole welding test. The welding tests lasted from 30 to 84 seconds.

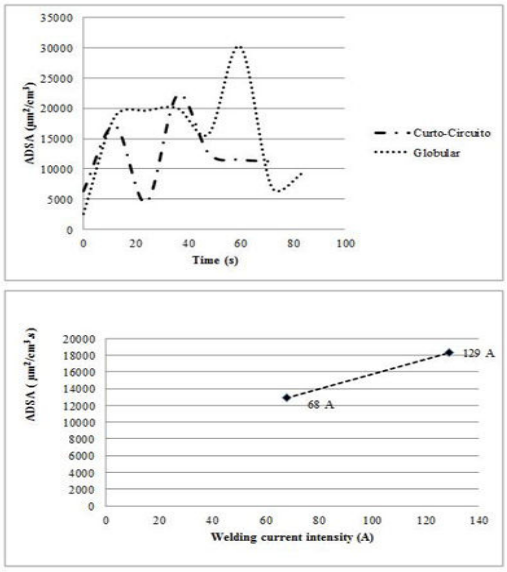


Fig. 4. Results for welding tests with 100% $CO_2$.

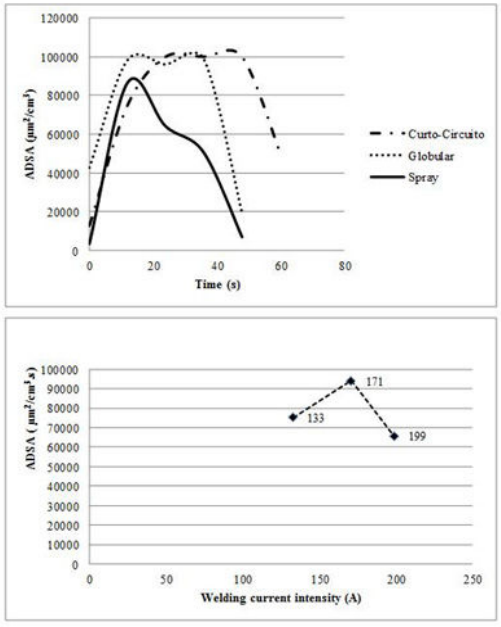


Fig. 5. Results for welding tests with ARCAL 121.

It can be easily seen that both the applied transfer modes and also the used gas mixtures have marked influence on the nanoparticulate emissions. Table 5 shows the average ADSA values obtained for the welding tests with carbon steel. Using gas mixture ARCAL 21, spray transfer mode is the one that results in higher ADSA values, and he same occurs for the other gaseous mixtures: with increasing values of welding parameters, ADSA values are also higher. One could expect the highest ADSA values were obtained for 100% $CO_2$: however, this behaviour was not obtained for the later gaseous mixture but for ATAL, having only 18% $CO_2$.

Table 6 shows the average ADSA values obtained for stainless steel welding: again, ADSA values increase with higher current intensity values, except for ARCAL 121, which was to be expected, considering that the spray mode results in higher values than those with globular transfer mode.

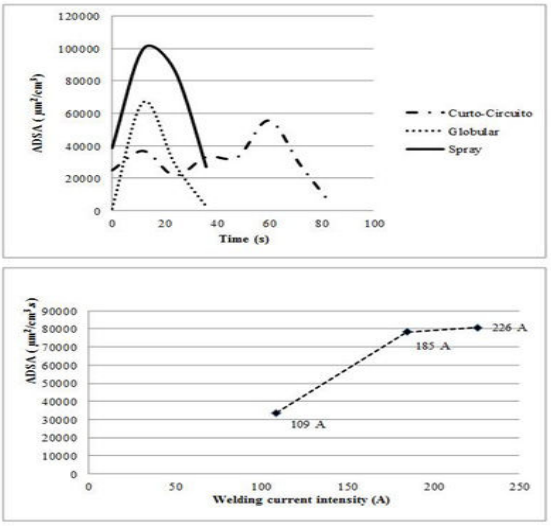


Fig. 6. Results for welding tests with ARCAL 129.

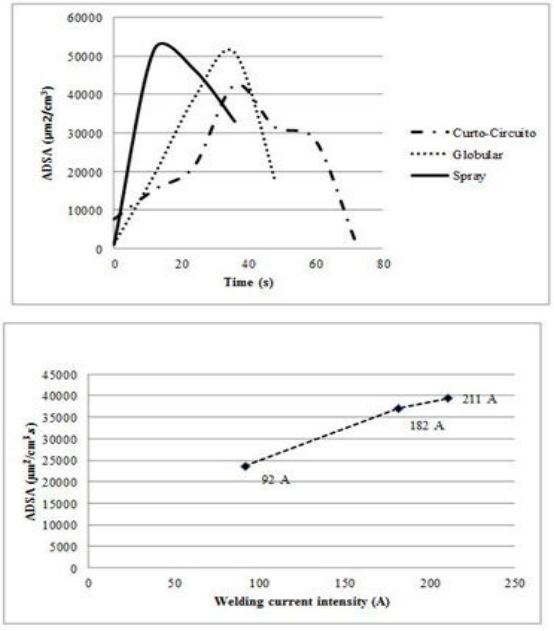


Fig. 7. Results for welding tests with ARCAL 12.

This could be due to the welding parameters tested: possibly the used current intensity (199 A) falls into a zone (in terms of electric arc strenght and electric arc

current, as depicted in figure 8) corresponding to a low fume emission rate [17].

The overall result is a lower value when compared to the other transfer modes.

In fact, ARCAL 121 is the gaseous mixture resulting in higher emissions of nanoparticles, as measured by ADSA. Another possible cause for this is related with the high content of He in the gaseous mixture (18%): as He exhibits a very high ionization energy value of 24.58 eV, this will result in an electric arc having higher temperatures capable of producing a higher volatilization of elements both from the base material and the consumable.

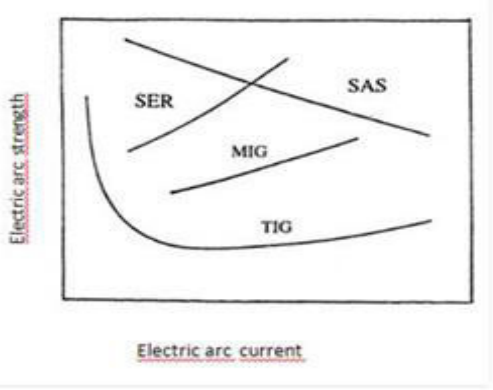


Fig. 8. Relation between electric arc strength and current for different welding processes [17].

Table 5. Average ADSA values obtained during welding tests for mild steel

| Gas mixture | Average ADSA ($\mu m^2/cm^3.s$) | | |
|---|---|---|---|
| Metal transfer mode | ARCAL 21 | ATAL 5 | 100% $CO_2$ |
| Short-circuit | 8325 | 22266 | 12899 |
| Globular | 13306 | 42896 | 18292 |
| Spray | 17574 | - | - |

Table 6. Average ADSA values obtained during welding tests for stainless steel

| Gas mixture | Average ADSA ($\mu m^2/cm^3.s$) | | |
|---|---|---|---|
| Metal transfer mode | ARCAL 129 | ARCAL 121 | ARCAL 12 |
| Short-circuit | 23637 | 75390 | 33644 |
| Globular | 37054 | 94136 | 78361 |
| Spray | 39376 | 65829 | 80861 |

Comparing tables 5 and 6, it is also possible to note that higher ADSA values are obtained for welding stainless steel than carbon steel.

Figures 9 to 11 show the collected nanoparticles using the NAS equipment: figure 9 refers to welding carbon steel with ARCAL 21 and figures 10 and 11 refer to welding stainless steel with ARCAL 121 and ARCAL 129, respectively.

Nanoparticles shown in figures 9 are spherical, amorfous and with dimensions ranging from 10 to 90 nm, and are aggregated together. Also regarding stainelss steel welding, nanoparticles are spherical and amorfous, agglomerated, with dimensions ranging from 10 to 40 nm.

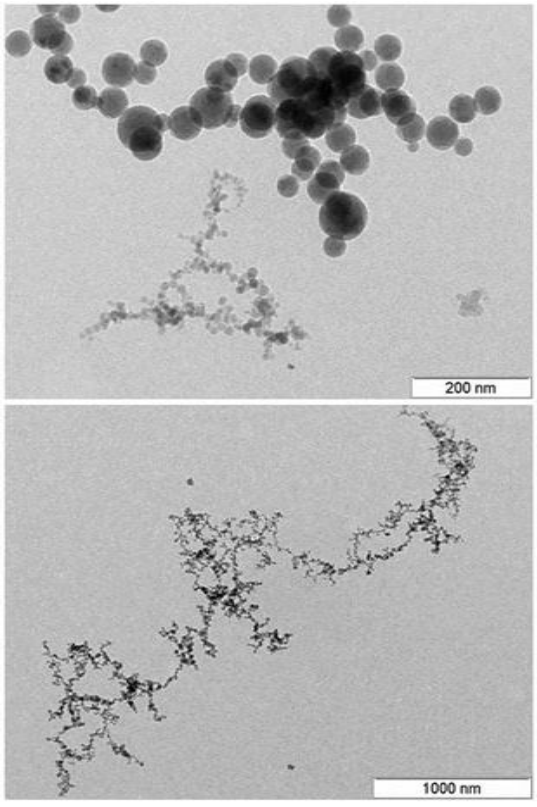


Fig. 9. TEM image for nanoparticles collected for welding with ARCAL 21.

The particles were subjected to chemical analysis, by EDS, and the obtained spectra are shown in figures 12 and 13, for carbon steel (ARCAL 21) and for stainless steel (ARCAL 129), respectively.

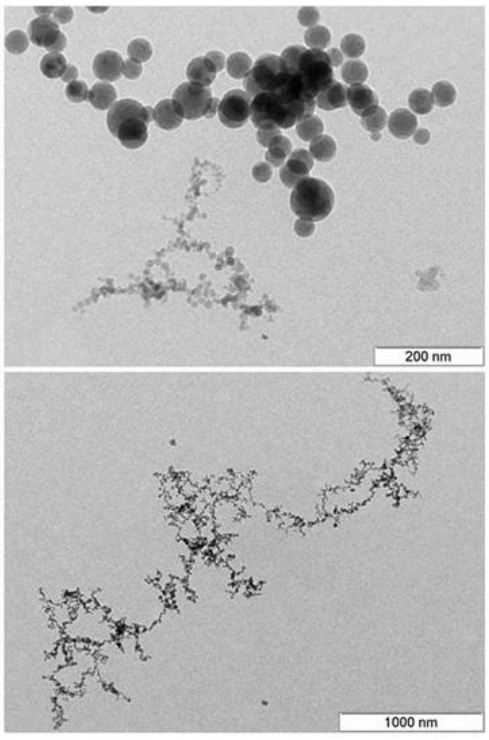


Fig. 10. TEM image for nanoparticles collected for welding with ARCAL 121.

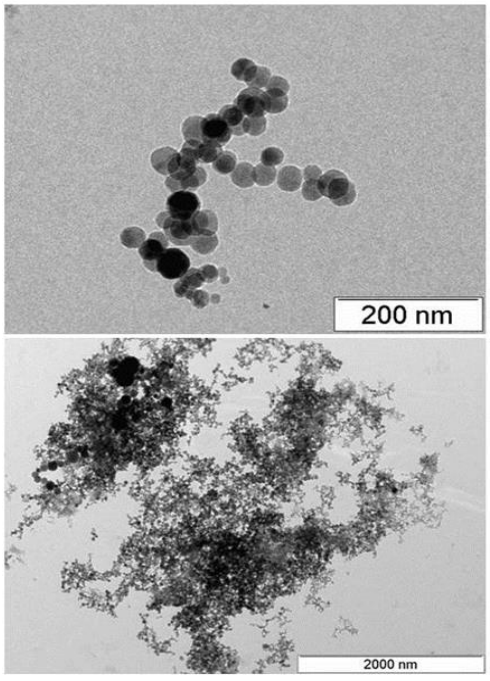


Fig. 11. TEM image for nanoparticles collected for welding with ARCAL 129.

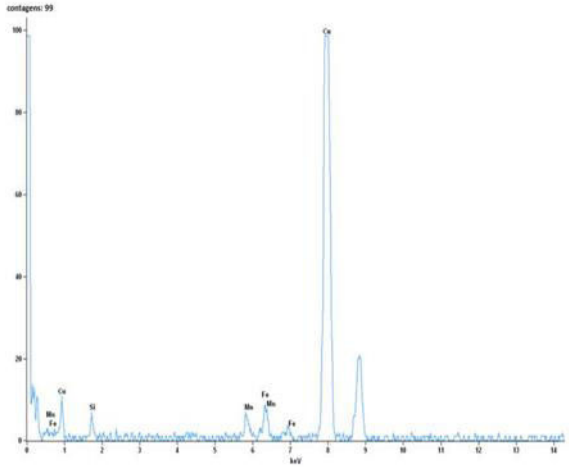

Fig. 12. Chemical composition of nanoparticles collected for welding with ARCAL 21.

Regarding carbon steel, the elements detected were iron, silicium and manganese (copper is also shown in the spectra but it is due to the grids used for collecting nanoparticles). For stainless steel, the detected elements were iron, cromium and nickel, which confirms the origin both from the base material and also the consumable.

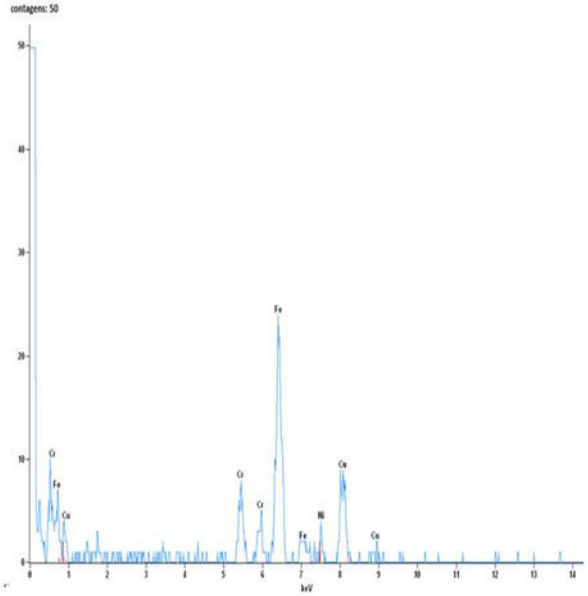

Fig. 13. Chemical composition of nanoparticles collected for welding with ARCAL 129.

## 4. Conclusions

From this work the following conclusions can be derived:
i) the nanoparticles emission, as measured by ADSA, increases with the increase of welding parameters such as current intensity and tension;
ii) regarding the studied transfer modes, the spray mode is the one resulting in higher emissions of nanoparticles;
iii) the short-circuit mode resulted in lower average ADSA values for all gaseous mixtures tested. It should be noted that this transfer mode exhibits the lowest current intensity and tension, resulting in lower temperatures of the electric arc thus volatilizing lower quantities of elements from the base materials and consumables;
iv) globular transfer mode, for the majority of tested conditions, results in ADSA values between short-circuit and spray modes. This transfer mode is known by creating instability in the electric arc and, thus, it seems that electric arc instability is not the main cause for nanoparticles emission but, instead, the electric arc temperature;
v) regarding carbon steel welding, the gaseous mixture composed by 82% Ar+18% $CO_2$ resulted in high ADSA values, which was somewhat unexpected, as previous studies on fume emissions showed that the fume formation increased with the increase of $CO_2$ presence in the gaseous mixture;
vi) concerning stainless steel, the gaseous mixture composed by 81% Ar+18% He+1% CO2 resulted in high ADSA values, which seems to result from the high quantity of He in the mixture. As He has a high ionization energy, the resulting electric arc has higher temperatures which produces a higher volatilization of elements both from base material and consumable;
vi) comparing the base materials used, it should be noted that higher ADSA values were obtained for stainless steel when compared to carbon steel. Also, the emitted nanoparticles for stainless steel showed the presence of nickel and chromium which are potentially carcinogenic elements;
vii) the collected particles, both for carbon steel and stainless steel have nanometric dimensions, the majority between 10 and 100 nm.

## Acknowledgements

The authors acknowledge the support of Fundación MAPFRE, Madrid, Spain through a Beca I. Hernando de Larramendi. The authors also thank Ms. Catarina Pereira and Mr. António Campos, Miguel Bento and Tiago Pereira, who assisted in performing the welding tests. The authors also thank Dr. Telmo Santos, from FCT-UNL, who helped with the data analysis and Dr. Patrícia Carvalho, from Microlab-IST, who performed the electronic microscopy analysis.

## References

[1] J. Gomes, Higiene e Segurança da Soldadura, ISQ, Oeiras, 1983 (in Portuguese).
[2] I. Pires, L. Quintino, R. Miranda, J. Gomes, Tox. Env. Chem. 88, 385 (2006).
[3] C. Ascenço, J. Gomes, N. Cosme, R. Miranda, Tox. Env. Chem. 87, 345 (2005).
[4] J. Gomes, P. Albuquerque, R. Miranda, M. Vieira, J. Tox. Env. Health - A 75, 747 (2012).
[5] N. Jenkins, T. Eager, Weld. J., Supp. 87 (2005).
[6] J. Dasch, J. D'Arcy, J. Occ. Env. Hyg. 5, 444 (2008).
[7] G. Buonanno, L. Morawska, L. Stabile, J. Aer. Sci. 42, 295 (2011).
[8] B. Moroni, C. Viti, Aer. Sci. 40, 938 (2011).
[9] K. Elihn, P. Berg, G. Liden,, J. Aer. Sci. 42, 127 (2011).
[10] G. Oberdörster, R. Gelein, J. Ferin, B. Weiss, Inh. Tox. 7, 111 (1995).
[11] D. Rickerby, M. Morrison, Sci. Tech. Adv. Mat. 8, 19 (2007).
[12] G. Oberdörster, Int. Arch. Occ. Env. Health 74, 1 (2001).
[13] W. Kreyling, M. Semmler, F. Erbe, P. Mayer, S. Takenaka, H. Schulz, G. Oberdörster, A. Ziesenis, J. Tox. Env. Health – A 65, 511 (2002).
[14] R. Phalen, Particle Size-selective sampling for particulate air contaminants, Ed. J.H. Vincent, ACGIH, Cincinnati, 1999.
[15] J. Gomes, P. Albuquerque, R. Miranda, T. Santos, M. Vieira, Inh. Tox. 24, 774 (2012).
[16] B. Berlinger, N. Benker, S. Weinbruch, B. L'Vov, M. Ebert, W. Koch, D. Ellingsen, Y. Thomassen, Anal. Bioanal. Chem. 399, 1773 (2009).
[17] I. Pires, L. Quintino, R. Miranda, Mat. Des. 28, 1623 (2007).
[18] O. Santos, L. Quintino, Processos de soldadura, ISQ, Lisboa, 1999 (in Portuguese).